Critical behavior of heat capacity at the smectic-C_α^*–smectic-A transition of the antiferroelectric liquid crystal methylheptyloxycarbonylphenyl octyloxybiphenyl carboxylate (MHPOBC)

Kenji Ema, Jun Watanabe, Atsushi Takagi, and Haruhiko Yao
Department of Physics, Faculty of Science, Tokyo Institute of Technology, 2-12-1 Oh-okayama, Meguro-Ku, Tokyo 152, Japan
(Received 21 February 1995)

High resolution ac calorimetric measurements have been carried out near the smectic-C_α^*–smectic-A phase transition in an antiferroelectric liquid crystal 4-(1-methylheptyloxycarbonyl)phenyl 4′-octyloxybiphenyl-4-carboxylate. A clear deviation from the extended mean-field Landau behavior was seen. The data have been analyzed using a renormalization-group expression, including the correction-to-scaling terms. It was found that the heat-capacity anomaly is described well with the three-dimensional XY model, in agreement with the theoretical prediction. It was also found that the second-order correction terms play quite an important role.

PACS number(s): 64.70.Md, 61.30.−v, 64.60.Fr, 65.20.+w

Theoretically, the smectic-A (Sm-A)–smectic-C (Sm-C) transition and the smectic-A–chiral-smectic-C (Sm-C^*) transition belong to the three-dimensional (3D) XY universality class [1]. On the other hand, experimentally observed data on the heat capacity, the tilt order parameter, the susceptibility etc. at these transitions are well-described by the extended Landau theory which includes up to sixth-order term of the tilt order parameter (see Refs. [2–5], and also references therein) with only a few exceptions [6,7]. Recently, the present authors [8] measured the heat capacity of 4-(1-methylheptyloxycarbonyl)phenyl 4′-octyloxybiphenyl-4-carboxylate (MHPOBC), which exhibits paraelectric Sm-A, antiferroelectric Sm-C_α^*, ferroelectric Sm-C^*, ferrielectric Sm-C_γ^*, and antiferroelectric Sm-C_A^* phases with decreasing temperature [9]. It was found that the heat-capacity anomaly accompanying the Sm-C_α^*–Sm-A transition in MHPOBC is roughly explained by the same extended Landau theory as mentioned above. However, as noticed from Fig. 1 of Ref. [8], excess heat capacity is seen in the Sm-A phase over several degrees, while no excess heat capacity is expected in the disordered phase within the framework of the extended Landau theory. In this paper we report the results of our most recent ac calorimetric measurement on MHPOBC with improved precision, and detailed analyses of the observed anomaly. The results described below will show that the anomaly is not explained by the extended Landau theory. Further, the anomaly can be fitted well with the 3D XY model, in agreement with the theoretical prediction [1].

The ac calorimeter used is basically the same as described in our previous work [8,10], except that some modifications have been made to improve the resolution of the measurement. The sample temperature is measured with an ac-driven Wheatstone bridge using a lock-in amplifier (Princeton Applied Research 5209) and an arbitrary waveform generator (Biomation 2411A). The bath temperature is monitored with a precision thermometry bridge (F700A, Automatic System Laboratory, UK). This lineup enables us to obtain heat-capacity data with a precision of about ±0.015% (this value quotes the standard deviation in the total heat capacity including that of the empty cell). The scan rate of the sample temperature is slightly less than 1 mK/min near the transition temperature.

Figure 1 shows the temperature dependence of the excess heat capacity ΔC_p obtained on cooling. A normal part of the heat capacity linearly dependent on the temperature has been subtracted so that the excess part goes smoothly to zero at temperatures far away from the transition on the both sides. Identical results were obtained in other runs irrespective of heating or cooling, except a very small shift in the temperature scales due to the drift in transition temperatures with a rate of about −0.005 K/day. The peak at the Sm-C_α^*–Sm-A transition is quite sharp, with a very narrow rounding region of about 20 mK. The existence of excess heat capacity in the Sm-A phase is quite clear. We also note that two of the three restructuring transitions, Sm-C_γ^*–Sm-C^*, and Sm-C^*–Sm-C_α^*, are now visible, with very small anomalies of about 0.003 J/gK and 0.010 J/gK, respectively.

Whether the present data are really incompatible with the extended Landau theory should be examined very

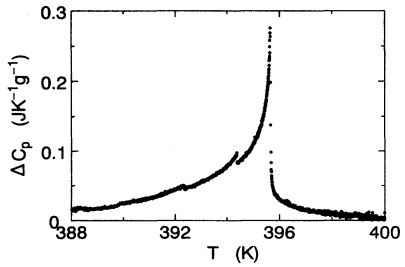

FIG. 1. Detailed view of the excess heat capacity near the Sm-C_α^*–Sm-A phase transition of MHPOBC. The anomalies at about 392.3 K and 394.4 K correspond to the Sm-C_γ^*–Sm-C^* and the Sm-C^*–Sm-C_α^* transitions, respectively.

carefully. Qualitatively similar C_p tails above T_c (the corresponding Sm-C–Sm-A or Sm-C^*–Sm-A transition temperature will be called T_c, hereafter) have been reported for several cases, but usually they were ascribed to be caused by inhomogeneities or impurities in the sample [4]. In such cases the experimental C_p curves exhibit rounded maxima and drop to the baseline over a narrow temperature range of typically less than a few tenths of a degree [11]. If the tail observed for MHPOBC was caused by a similar extrinsic origin, we should expect that the sample quality is relatively low because the tail extends over a wide temperature range as seen in Fig. 1. On the contrary, the high quality of the MHPOBC sample is guaranteed by the sharpness of the restructuring transitions between the chiral smectic-C phases with two-phase coexistence ranges of only about 10 mK [8]. Therefore, it is very unlikely that the MHPOBC sample had inhomogeneities or impurities which can explain the C_p tail observed here.

In addition to the existence of excess heat capacity above T_c described above, the critical nature of the anomaly observed here is most directly seen in Fig. 2, where $(\Delta C_p/T)^{-2}$ is plotted against the temperature. This plot should be a straight line for the data below T_c according to the extended Landau free energy expressed as

$$G = G_0 + a'(T - T_0)\phi^2 + b\phi^4 + c\phi^6, \qquad (1)$$

where G_0 is the normal part of the free energy, ϕ is the tilt order parameter, and a', b, c, T_0 are constants [2]. Thus the downward bending of the curve just below T_c seen in Fig. 2 shows that the increase in ΔC_p is steeper than predicted by the extended Landau theory. Including higher-order terms (ϕ^8, or higher) only makes the curve bend upward at low temperatures because the order parameter saturates faster in that case, but does not explain the above disagreement. We tried other physically acceptable choices of the baseline in obtaining the excess part, but the result was the same for all cases. Also, we are free from ambiguity in determining the extrapolated unstable point T_m [2], because in Fig. 2 the plot has been made on a linear temperature scale instead of a logarithmic scale. A similar increase in ΔC_p steeper than the prediction of the mean-field theory below T_c was found in one of the samples of p-(n-decyloxybenzylidene)-p-amino-(2-methylbutyl) cinnamate (DOBAMBC) studied by Dumrongrattana *et al.* [12]. They pointed out the possibility that it was due to impurities because such an increase was not seen in another sample they studied which showed a sharper peak. However, the rounding in our data is much narrower than in their *better* sample (roughly estimating from Fig. 3 of Ref. [12], the rounding width is slightly less than 0.1 K in their case, which is about four times wider than ours). We could also mention the extremely slow T_c drift rate (−0.005 K/day) as another support of the quality of MHPOBC, which is an order of magnitude smaller than in DOBAMBC (−2 mK/h = −0.048 K/day). In view of the points discussed above, we conclude that the ΔC_p data obtained for MHPOBC are incompatible with the extended Landau theory.

Our next issue is to determine the universality class to which the present critical heat capacity belongs. For this purpose, the C_p data have been analyzed with the following renormalization-group expression including the corrections-to-scaling terms [13]:

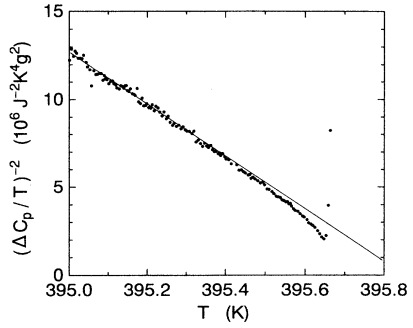

FIG. 2. Plot of $(\Delta C_p/T)^{-2}$ against T. Solid line is a guide to the eye.

$$\Delta C_p = A^{\pm}|t|^{-\alpha}\left(1 + D_1^{\pm}|t|^{\Delta_1} + D_2^{\pm}|t|\right) + B_c, \qquad (2)$$

where $t \equiv (T - T_c)/T_c$ is the reduced temperature, and the superscripts $\pm$ denote above and below T_c. The second-order correction term $D_2^{\pm}|t|$ is actually a combination of several higher-order terms that have almost the same t dependence [14,15]. In general, ΔC_p peak is more or less rounded in the immediate vicinity of T_c. The extent of the rounding region was carefully determined in the way described elsewhere [16], and the data inside this region were excluded in the fitting. Typically, the rounding region thus determined is $-3\times10^{-5} < t < +1\times10^{-5}$.

At first, the exponent α was adjusted freely in the least-squares calculation. The correction-to-scaling exponent Δ_1 is actually system dependent, but has a value quite close to 0.5 as far as theoretically known (0.524 for 3D XY, and 0.496 for 3D Ising model [13]). Therefore, we fixed its value to 0.5 in this stage of fitting. The coefficients $D_2^{\pm}$ were held fixed at zero. Fits were made for the data over three ranges, $|t|_{\max}$=0.0025, 0.001, and 0.0005, where $|t|_{\max}$ is the maximum value of $|t|$ used in the fit. Larger $|t|_{\max}$ were not tried since the small but discernible anomaly accompanying the restructuring transitions might affect the fitting. In Table I, the first three lines show the values of the critical exponent α, the critical amplitude ratio A^-/A^+, and other adjustable parameters thus obtained. The values of the universal constant $R_B^+ \equiv A^+|D_1^+|^{\alpha/\Delta_1}B_c^{-1}$ are also shown. It is seen that the fits yield an α close to the 3D Ising value of 0.11, rather than the 3D XY value of −0.0066 [13].

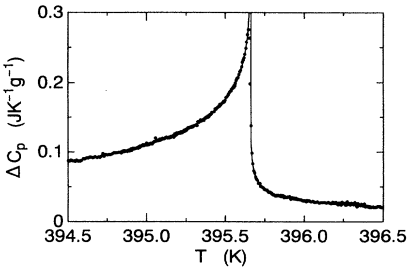

FIG. 3. Comparison of the observed data (closed circles) and the 3D XY fitting curve (solid line).

TABLE I. Least-squares values of the adjustable parameters for fitting ΔC_p with Eq. (2). Quantities in brackets were held fixed at the given values. In the 3D XY and 3D Ising fits, the exponent Δ_1 has been held fixed to the theoretical values. The units for A^+ and B_c are $\mathrm{J\,K^{-1}\,g^{-1}}$.

$\lvert t\rvert_{\max}$	T_c (K)	α	A^+	A^-/A^+	D_1^+	D_1^-	B_c	R_B^+	χ_ν^2
0.0025	395.667	0.15	0.0228	3.286	-1.237	-6.48	-0.0326	-0.584	1.43
0.0010	395.665	0.09	0.0951	1.963	3.45	-4.28	-0.1670	-0.743	0.95
0.0005	395.665	0.09	0.0932	1.982	3.04	-3.03	-0.1617	-0.742	1.04
0.0025	395.648	[-0.0066]	-4.566	0.960	-0.292	0.300	4.3564	-1.065	4.07
0.0010	395.655	[-0.0066]	-4.989	0.959	-0.422	0.348	4.7436	-1.063	1.37
0.0005	395.657	[-0.0066]	-5.117	0.958	-0.480	0.380	4.8596	-1.062	1.07
0.0025	395.664	[0.110]	0.0610	2.203	2.65	-4.21	-0.1128	-0.712	1.62
0.0010	395.666	[0.110]	0.0564	2.354	2.67	-5.15	-0.1019	-0.735	0.96
0.0005	395.665	[0.110]	0.0595	2.252	2.41	-4.45	-0.1095	-0.684	1.06

We next fitted the data fixing the exponents α and Δ_1 to theoretically expected values for 3D XY and 3D Ising models. The fourth through ninth lines in Table I show the results of such fits. In both Ising and XY fits, values of A^-/A^+ and R_B^+ are stable against the data range shrinking. Values of $D_1^\pm$ seem reasonable in the sense that they are of the order of unity, although the theoretical prediction that $D_1^+ = D_1^-$ [17] is not fulfilled. The agreement of the universal constants A^-/A^+ and R_B^+ with the theoretical values is excellent for the XY case ($A^-/A^+ = 0.971$ and $R_B^+ = -1.057$ [18]), while it is slightly worse for the Ising case ($A^-/A^+ = 1.848$ and $R_B^+ = -0.708$ [13]). As for the fit quality judged from the χ_ν^2 values, the XY and Ising fits are almost the same for $\lvert t\rvert_{\max}$=0.0005, while the Ising fit seems clearly favorable for $\lvert t\rvert_{\max}$=0.0025. However, it should be noted that χ_ν^2 increases considerably as the value of $\lvert t\rvert_{\max}$ is increased, suggesting the importance of the second-order correction terms.

Table II shows the results of the fitting when the second-order correction terms are included. The results for $\lvert t\rvert_{\max}$=0.0005 are omitted here because it was found that the fitting region was too narrow to get a reliable estimation of $D_2^\pm$ values. It is seen that XY and Ising fits are of equal quality in the χ_ν^2 sense even for the widest data range. The exponent α, when adjusted freely, lies between XY and Ising values. However, physical significance of the parameter values favors the 3D XY model first because the agreement of A^-/A^+ and R_B^+ with the theoretical values is clearly better, and also because the $D_2^\pm$ values seem rather large and are unstable against $\lvert t\rvert_{\max}$ in the case of the Ising fit. Figure 3 shows the theoretical fit with 3D XY exponents to the data with $\lvert t\rvert_{\max} = 0.0025$. It is seen that the agreement between the observed and theoretically calculated values is fairly good. After all, we can say that the observed C_p anomaly is described adequately with the 3D XY model, in agreement with the theoretical expectation. It deserves attention that the second-order correction terms play a significant role in the present case. This reflects the fact that the asymptotic critical region is narrower in MHPOBC than in other 3D XY transitions such as the Sm-A to nematic phase in liquid crystals (see Ref. [15], and references therein). On the other hand, it is difficult at this moment to exclude out the 3D Ising model because the difference is rather small. Therefore, attempts should be made to determine other critical indices to obtain more definite and universal understanding of the critical behavior in this substance.

An issue that needs further discussion is why critical behavior is seen in MHPOBC and not in almost all other liquid crystals which also undergo the Sm-C(or Sm-C^*)–Sm-A phase transition. One might argue that this is specific to the antiferroelectricity or more particularly antiferroelectric Sm-C_α^* phases. In crystalline uniaxial dipolar systems, it is known that the long-range dipolar interaction suppresses the critical fluctuation and changes the upper critical dimensionality from four to three in case of ferromagnets or ferroelectrics, whereas it *does not* in antiferromagnets or antiferroelectrics [19]. Since the Sm-C_α^* phase of MHPOBC disappears in optically impure systems [20], it is expected that the dipolar interaction plays an important role in this transition. Nevertheless, a question arises why such a critical behavior is not observed in MHPOCBC [8], which is the octyloxycarbonylbiphenyl analog of MHPOBC, and also exhibits antiferroelectric

TABLE II. Least-squares values of the adjustable parameters for fitting ΔC_p with Eq. (2). Quantities in brackets were held fixed at the given values. In the 3D XY and 3D Ising fits, the exponent Δ_1 has been held fixed to the theoretical values. The units for A^+ and B_c are $\mathrm{J\,K^{-1}\,g^{-1}}$.

$\lvert t\rvert_{\max}$	T_c (K)	α	A^+	A^-/A^+	D_1^+	D_1^-	D_2^+	D_2^-	B_c	R_B^+	χ_ν^2
0.0025	395.664	0.05	0.3340	1.422	4.60	-2.58	-37.6	17.1	-0.4932	-0.581	1.22
0.0010	395.664	0.05	0.3329	1.423	4.75	-2.44	-42.4	12.6	-0.4919	-0.579	0.94
0.0025	395.659	[-0.0066]	-5.467	0.958	-0.741	0.442	5.63	-3.45	5.1787	-1.060	1.24
0.0010	395.661	[-0.0066]	-5.500	0.956	-0.857	0.535	7.80	-4.97	5.2043	-1.059	0.94
0.0025	395.666	[0.110]	0.0609	2.287	6.13	-4.87	-51.2	15.1	-0.1202	-0.757	1.30
0.0010	395.666	[0.110]	0.0572	2.312	1.93	-4.68	19.6	-10.0	-0.1031	-0.642	0.96

Sm-C^*_α phase [21]. In this connection, the comparison of the data on MHPOBC, MHPOBCBC, and also MHPBC, which is the octylbiphenyl analog of MHPOBC [22], is of interest. All these three undergo the same Sm-C^*_α–Sm-A phase transition, and the C_p anomaly becomes smaller in the order of MHPOBC, MHPBC, and MHPOCBC, the peak height of the anomaly in MHPOCBC being about one sixth of that in MHPOBC. The tail in the Sm-A phase is clear in MHPOBC, while it is hardly seen in MHPOCBC. In case of MHPBC, the tail is still visible but smaller than in MHPOBC [23]. A universal understanding of the transitions in these substances will give light to the origin of the critical behavior observed in MHPOBC. Another key will be found through the measurements on other related physical quantities. Using the Ginzburg criterion, Safinya *et al.* [24] argued that the bare correlation length characterizing the tilt fluctuations is generally large for most Sm-A–Sm-C transitions so that the true critical region should be unobservably small. Based on the same picture, it is expected that the bare correlation length for MHPOBC is comparatively small. Measurements of correlation length will clarify this point. Also, measurements on other antiferroelectric liquid crystals will be quite helpful.

We wish to thank Professor H. Takezoe for supplying us high-quality MHPOBC samples and also for helpful discussions.

[1] P. G. de Gennes, Mol. Cryst. Liq. Cryst. **21**, 49 (1973).
[2] C. C. Huang and J. M. Viner, Phys. Rev. A **25**, 3385 (1982).
[3] C. C. Huang and S. Dumrongrattana, Phys. Rev. A **34**, 5020 (1986).
[4] T. Chan, Ch. Bahr, G. Heppke, and C. W. Garland, Liq. Cryst. **13**, 667 (1993).
[5] F. Yang, G. W. Bradberry, and J. R. Sambles, Phys. Rev. E **50**, 2834 (1994).
[6] The work by M. Delaye, J. Phys. (Paris) **40**, C3-350 (1979), on *p*-nonyoxybenzoate-*p*-butyloxyphenol revealed critical behavior and small bare correlation length, which seem to be consistent with each other.
[7] As for recent arguments on azoxy-4, 4'-di-undecyl-α-methylcinnamate (AMC-11), see Y. Galerne, J. Phys. (Paris) **46**, 733 (1985); G. Nounesis, C. C. Huang, T. Pitchford, E. Hobbie, and S. T. Lagerwall, Phys. Rev. A **35**, 1441 (1987).
[8] K. Ema, H. Yao, I. Kawamura, T. Chan, and C. W. Garland, Phys. Rev. E **47**, 1203 (1993).
[9] A. D. L. Chandani, Y. Ouchi, H. Takezoe, A. Fukuda, K. Terashima, K. Furukawa, and A. Kishi, Jpn. J. Appl. Phys. **28**, L1261 (1989); Y. Takanishi, K. Hiraoka, V. K. Agrawal, H. Takezoe, A. Fukuda, and M. Matsushita, *ibid.* **30**, 2023 (1991); K. Hiraoka, Y. Takanishi, K. Skarp, H. Takezoe, and A. Fukuda, *ibid.* **30**, L1819 (1991).
[10] K. Ema, T. Uematsu, A. Sugata, and H. Yao, Jpn. J. Appl. Phys. **32**, 1846 (1993).
[11] J. Boerio-Goates, C. W. Garland, and R. Shashidhar, Phys. Rev. A **41**, 3192 (1990), and references therein.
[12] S. Dumrongrattana, C. C. Huang, G. Nounesis, S. C. Lien, and J. M. Viner, Phys. Rev. A **34**, 5010 (1986).
[13] C. Bagnuls and C. Bervillier, Phys. Rev. B **32**, 7209 (1985); C. Bagnuls, C. Bervillier, D. I. Meiron, and B. G. Nickel, Phys. Rev. B **35**, 3585 (1987).
[14] C. Bagnuls and C. Bervillier, Phys. Lett. **112A**, 9 (1985).
[15] C. W. Garland, G. Nounesis, M. J. Young, and R. J. Birgeneau, Phys. Rev. E **47**, 1918 (1993).
[16] H. Haga, A. Onodera, Y. Shiozaki, K. Ema, and H. Sakata, J. Phys. Soc. Jpn. **64**, 822 (1995).
[17] A. Aharony and G. Ahlers, Phys. Rev. Lett. **44**, 782 (1980).
[18] C. Bervillier, Phys. Rev. B **34**, 8141 (1986).
[19] A. Aharony, Phys. Rev. B **8**, 3349 (1973); **8**, 3363 (1973).
[20] H. Takezoe, J. Lee, A. D. L. Chandani, E. Gorecka, Y. Ouchi, A. Fukuda, K. Terashima, and K. Furukawa, Ferroelectrics **114**, 187 (1991).
[21] T. Isozaki, Y. Suzuki, I. Kawamura, K. Mori, N. Yamamoto, Y. Yamada, H. Orihara, and Y. Ishibashi, Jpn. J. Appl. Phys. **30**, L1573 (1991); T. Isozaki, K. Hiraoka, Y. Takanishi, H. Takezoe, A. Fukuda, Y. Suzuki, and I. Kawamura, Liq. Cryst. **12**, 59 (1992).
[22] N. Okabe, Y. Suzuki, I. Kawamura, T. Isozaki, H. Takezoe, and A. Fukuda, Jpn. J. Appl. Phys. **31**, L793 (1992).
[23] K. Ema, J. Watanabe, and H. Yao, Ferroelectrics **156**, 173 (1994).
[24] C. R. Safinya, M. Kaplan, J. Als-Nielsen, R. J. Birgeneau, D. Davidov, J. D. Litster, D. L. Johnson, and M. E, Neubert, Phys. Rev. B **21**, 4149 (1980).